Journal of Materials Chemistry A

Creating Robust Superamphiphobic Coatings for Both Hard and Soft Materials

Journal:	*Journal of Materials Chemistry A*
Manuscript ID	TA-ART-07-2015-005333.R1
Article Type:	Paper
Date Submitted by the Author:	01-Sep-2015

Complete List of Authors:	Chen, Faze; Dalian University of Technology, School of Mechanical Engineering Song, Jinlong; Dalian University of Technology, School of Mechanical Engineering Lu, Yao; University College London, Department of Chemistry Huang, Shuai; Dalian University of technology, School of Mechanical Engineering Liu, Xin; Dalian University of technology, School of Mechanical Engineering Sun, Jing; Dalian University of technology, School of Mechanical Engineering Carmalt, Claire; University College London, Department of Chemistry Parkin, Ivan; University College London, Department of Chemistry Xu, Wenji; Dalian University of technology, School of Mechanical Engineering

Journal Name

ARTICLE

Creating Robust Superamphiphobic Coatings for Both Hard and Soft Materials

Received 00th January 20xx,
Accepted 00th January 20xx

DOI: 10.1039/x0xx00000x

www.rsc.org/

Faze Chen[a], Jinlong Song[a]*, Yao Lu[b], Shuai Huang[a], Xin Liu[a], Jing Sun[a], Claire J. Carmalt[b], Ivan P. Parkin[b], Wenji Xu[a]*

Most superhydrophobic surfaces lose their water-repellency when either contaminated by oily liquids or by being mechanically damaged. Superamphiphobic surfaces are ones that repel both oil and water. However, to date such surfaces are hampered by being mechanically weak. Robust superamphiphobic surfaces with highly water and oil repellent properties are desired for a wide range of environments. Reported herein is a superamphiphobic coatings fabricated by a facile deposition method and followed by a low surface energy materials modification. These coatings can be applied on both hard and soft materials to repel water, glycerol, peanut-oil droplets and some organic solvents. Falling sand abrasion, UV irradiation and aqueous media immersion were used to test the mechanical robustness and durability of the superamphiphobic coatings. A multi-cycle stretch/release test was developed to characterize the robustness of the self-cleaning soft materials. A coated rubber-bond retained both water and oil repellency even after 50 stretch/release cycles. These tests show that the superamphiphobic coatings have remarkable mechanical robustness and UV/aqueous media resistance and can be readily applied to a wide variety of materials to form self-cleaning surfaces that are extremely robust and durable even under intense strains.

1. Introduction

Nature offers many examples that have inspired researchers to minimize solid-liquid interfacial interactions to fabricate liquid repellent materials, such as the leaves of Lotus and Rice plants[1-3], the Namib Desert Beetle[4], water strider legs[5], etc.[6-8]. In the last two decades, superhydrophobic surfaces with water contact angles > 150 ° and sliding angles < 10 ° have attracted much attention due to their various applications in anti-fouling[9-11], anti-icing[12-20], self-cleaning[21-23], oil/water separation[22,24-26], corrosion resistance[27-29], surfaces patterning[30-32] and lab-on-chip systems[33-35]. However, most superhydrophobic surfaces are easily contaminated by oil[36], which greatly limits their practical applications in many environments. Compared with superhydrophobic surfaces, superamphiphobic surfaces - which repel both water and oil, are more likely to be used for water/oil proofing in an oily environment[37,38]. The repulsion of oil by a surface is much more difficult to achieve than water repellency, because most oils have low surface tension making it easier for oils to penetrate and wet a surface. In order to repel liquids with a wide range of surfaces tensions, surface micro-morphologies are required to be specially designed such as a re-entrant structure[36,38-45]. Tuteja *et al.*[38-40] employed electrospun fibers to demonstrate that design of re-entrant structures on an initially-oleophilic flat surface allows the construction of superamphiphobic surfaces with extreme non-wetting properties to water and various organic liquids. Zhao *et al.*[46] fabricated super-toner and ink-repellent superoleophobic surface by photolithographic technique followed by surface modification. Song *et al.*[42] constructed re-entrant micro/nanometer-scale rough structures on Al substrates by electrochemical etching and immersion in $[Ag(NH_3)_2]^+$ solution. The resulting surfaces showed superior oil repellency capacity with a peanut-oil contact angle of 160.0±2 °. Liu *et al.*[47] used a combinational method, including plasma etching, physical deposition and chemical etching, to construct a specific doubly re-entrant structure that enables very low liquid-solid contact fraction, and renders the surface super-repellent.

Among the aforementioned methods, superamphiphobic surfaces have only been prepared on one of several substrates, such as glass[43,44], metal[42,48] and fabrics[40,49]. Few reports have shown a general method to make superamphiphobic coatings both on hard (metal and glass) and soft/flexible (scouring pad, sponge, filter paper and rubber) substrates. Coating methods, such as dip-coating and spray-deposition, are other widely employed methods in the fabrication of liquid repellent surfaces[23,49-52]. Coatings can be

[a] Key Laboratory for Precision and Non-Traditional Machining Technology of Ministry of Education, Dalian University of Technology, Dalian 116024, China. E-mail address: wenjixu@dlut.edu.cn (Prof. W. J. Xu), songjinlong@dlut.edu.cn (Dr. J. L. Song).
[b] Materials Chemistry Research Centre, Department of Chemistry, University College London, 20 Gordon Street, London, WC1H 0AJ, UK

Electronic Supplementary Information (ESI) available: [details of any supplementary information available should be included here]. See DOI: 10.1039/x0xx00000x

easily applied onto various substrates, and the coated surfaces can also be easily repaired once the surfaces are damaged. However, the existing methods to fabricate superamphiphobic coatings are somewhat complicated. In addition, most of the liquid repellent coatings are obtained from pre-made sol, resins or suspension[49,53-56], the storage stability of these pre-made mixtures could be a potential problem. Thus, a facial method to fabricate superamphiphobic coatings that is easy-to-preserve and has long-term-stability is urgently needed.

Robustness and durability are important issues in non-wetting surfaces fabrication and practical application because the morphologies (e.g. micro/nano hierarchical roughness, re-entrant structures etc.) on those surfaces are very mechanically weak and sometimes being removed by simply touching with a tissue[57]. For example, Kulinich and co-workers[12-14] and Lazauskas *et al.*[16] found that the anti-icing performance of the ice-repellent surfaces deteriorate because the surface asperities undergo gradual mechanical damage during icing/deicing cycles. Boinovich *et al.*[20] designed a mechanically robust and durable superhydrophobic surface to achieve cyclic icing/deicing treatment. Thus, creating mechanically robust liquid-repellent surfaces is of great importance. Deng *et al.*[51,52] obtained robust super-liquid repellent coatings and investigated the mechanical resistance by sand abrasion tests. Sand grains (100 to 300 μm in diameter) impinged the surfaces from a height of 10 to ~40 cm. Moreover, according to Boinovich *et al.*[58] and Kulinich *et al.*[59], alkyl-group coated surfaces were supposed to gradually lose their (super)hydrophobicity upon long-term contact with aqueous media or even ice, because physicochemical processes (e.g., hydrolysis of hydrophobic molecules, growth of an oxide layer) occured. Therefore it is necessary to evaluate the chemical stability of liquid-repellent surfaces. UV irradiation and aqueous solutions immersion (or prolonged contact with aqueous media) are widely used to evaluate the chemical stability and durability of non-wetting surfaces[56,59-61]. Recently, it was found that commercial adhesives were effective to bond superhydrophobic coatings on both hard and soft materials with highly improved robustness[23], which points to be a new way to improve the robustness of super-liquid repellent coatings.

In this paper, we firstly used a facile chemical deposition and low surface energy modification to fabricate superamphiphobic powder. The powder was simply coated on hard, soft and stretchable/flexible materials via spray adhesives or double sided tape to make superamphiphobic surfaces. The coated surfaces showed excellent water, glycerol, peanut-oil and organic solvents repellences. Moreover, the coatings exhibited remarkable robustness and durability under falling sand abrasion, aqueous media immersion and UV exposure tests. We also developed a new multi-cycle stretch-release test to characterize the robustness of self-cleaning soft flexible materials. The treated rubber retained superamphiphobicity even after 50 cycles of stretch-release tests and it is believed that these coatings can be readily applied to the circumstances where self-cleaning is required under intense strains.

2. Experimental

2.1 Materials

Al plates (purity ≥ 99.9%) were purchased from the Dalian Aluminum Material Manufacturer (China). Perfluorooctanoic acid [PFOA, $CF_3(CF_2)_6COOH$, purity ≥ 96%] was purchased from Sigma-Aldrich (USA). Analytical-grade glycerol, diiodomethane, ethylene glycol, benzyl alcohol and $CuCl_2$ were purchased from Tianjin Kermel Chemical Reagent Co. (China). Peanut-oil was purchased from Luhua Co. (China). Glass slide and soft porous materials (scouring pad, sponge, filter paper and rubber) were

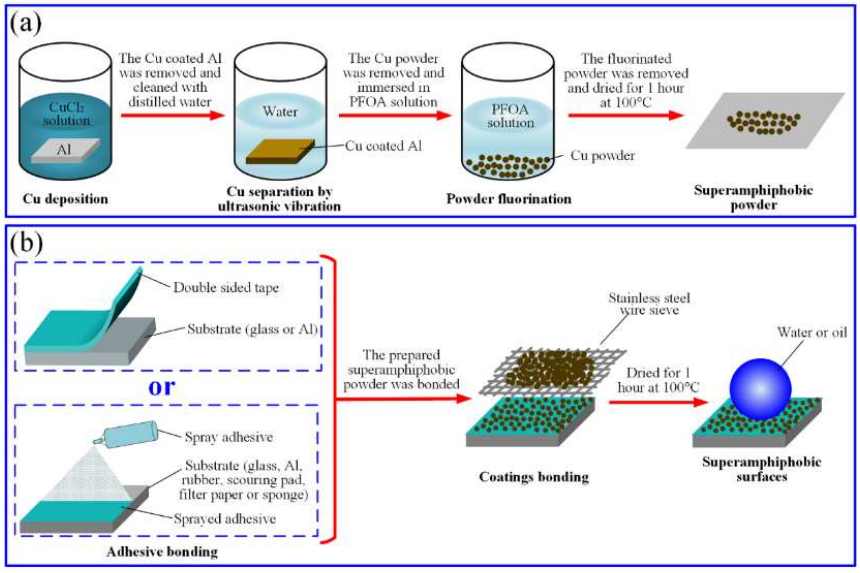

Fig. 1 Illustration of (a) the fabrication of the superamphiphobic powder and (b) the bonding of the powder onto various substrates.

purchased from Wal-Mart Stores in Dalian, China. Commercial adhesive, including the double sided tape (3M Scotch Brand Tape, core series 4-1000) and the spray adhesive (3M 77#), were purchased from 3M China. The surface tensions (γ_{LV}) of water, glycerol and peanut-oil are about 72.1 mN/m, 63.6 mN/m and 34.5 mN/m, respectively[51,62]. In the experiment, glycerol and peanut-oil were respectively dyed blue and yellow using oil blue and oil yellow to aid visualization, and this did not change the behavior of the droplets on the surfaces.

2.2 Fabrication of superamphiphobic coatings on both hard and soft materials

A simple chemical deposition and low surface energy modification was used to fabricate the superamphiphobic coatings as shown schematically in Fig. 1(a). Al plates were polished mechanically using 1000# and 2000# abrasive paper and then ultrasonically cleaned in sequence in alcohol and deionized water solvents. After drying in air, the Al plates were immersed in the 1 mol/L aqueous $CuCl_2$ solution at ambient temperature for 30 s to deposit a layer of Cu via a chemical substitution reaction. After immersion, the Cu-coated Al plates were thoroughly rinsed with deionized water to eliminate any residual salts and then the plates were ultrasonically cleaned with deionized water for 30 s to partially remove and refine the deposited dark red Cu. The separated Cu powder was then immersed in the 0.015 mol/L aqueous PFOA solution for 2 min to coat the powder and reduce its surface energy. Finally, the PFOA coated Cu powder was dried at 100 °C for 1 hour to obtain a superamphiphobic powder. Notably the obtained powder can be easily preserved in an air environment for more than 1 year without obvious loss of superamphiphobicity, and the samples are still under examination and measurements.

The superamphiphobic powder can be combined with spray adhesives or double sided tapes and easily coated on hard (Al and glass slide) and soft (rubber, scouring pad, sponge and filter paper) materials. After drying in air, the coated surfaces were noted to be superamphiphobic, as shown in Fig. 1(b).

2.3 Sample characterization

The crystal structures of the superamphiphobic powder were examined by X-ray diffractometer system (XRD-6000, Japan). The X-ray source was a Cu Kα radiation (λ = 0.15418 nm), which was operated at 40 kV and 40 mA with a scanning rate of 2θ = 0.026 deg/min and a range of 20–100 °. The chemical compositions of the powder was characterized by energy-dispersive X-ray spectroscope (EDS, INCA Energy, Oxford Instruments), and Fourier transform infrared spectrophotometer (FTIR, JASCO, Japan). The surface morphologies of the coated samples were observed by scanning electron microscope (SEM, JSM-6360LV, Japan). Contact angles (CAs) and roll-off angles (RAs) were measured by an optical contact angle meter (Krüss, DSA100, Germany) at room temperature by dropping droplets of 5 μL onto the coated surfaces and the average of five measurements obtained at different positions was used as the final CA/RA.

2.4 Surface robustness and durability tests

Falling sand abrasion tests were carried out to test the robustness of the superamphiphobic coatings on hard materials, and coated glass substrates were used as examples. 150 g of sand grains (300 to 800 μm in diameter) impinged the tilted surfaces (45 °) from different heights h (0 to ~100 cm, the corresponding velocities before impingement were 0 to ~4.47 m/s, see Supporting Information, Section S1). CAs and RAs were measured after each abrasion test. UV irradiation and solution immersion were conducted to test the chemical stability and the durability of the superamphiphobic coatings. To evaluate the UV resistance, the CAs and RAs of the superamphiphobic coatings after exposure to UV irradiation (365 nm, 32 W, see Supporting Information, Fig.S1) for 24 hours were measured. The resistance to distilled water, acidic, alkaline and saline solutions were tested by immersing completely coated glass substrates respectively in distilled water, 0.1 mol/L HCl, 0.1 mol/L NaOH and 0.5 mol/L NaCl aqueous solution for 24 h. A coated rubber-bond (~3.0 cm) was stretched to ~6.0 cm and then released (this process was defined as one cycle) to demonstrate the robustness of the superamphiphobic coatings on soft materials.

3. Results and discussion

Fig. 2(a) shows the XRD patterns of the superamphiphobic powder. Five diffraction peaks at 2θ = 43.28 °, 50.38 °, 74.12 °, 89.90 °, and 95.11 °, respectively, correspond to the characteristic peaks of the Cu(111), Cu(200), Cu(220), Cu(311), and Cu(222) planes of the face-centered cubic Cu crystals (JCPDS Card No. 04-0836). Reflections at 2θ = 29.48 °, 36.34 °, 42.39 ° and 61.43 ° matched the characteristic peaks of the Cu_2O(110), Cu_2O(111), Cu_2O(200) and Cu_2O(220) planes,

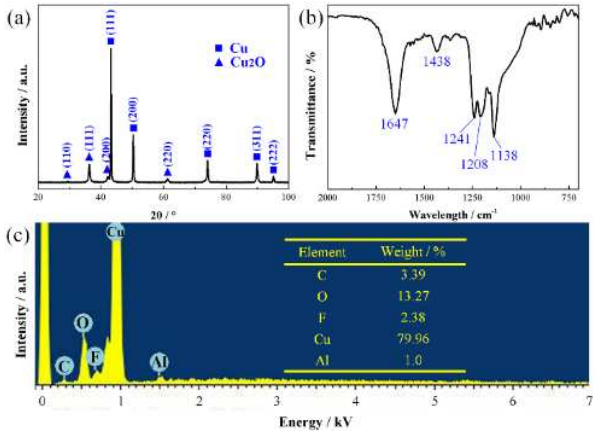

Fig. 2 (a) XRD patterns, (b) FTIR and (c) EDS spectra of the PFOA coated Cu/Cu_2O powder.

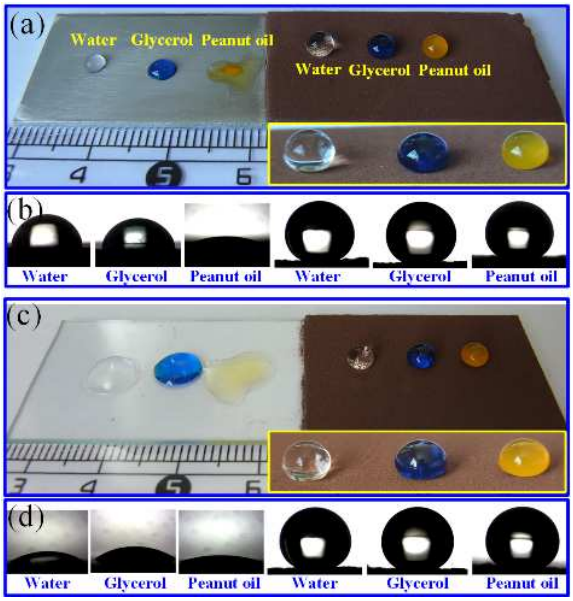

Fig. 3 Water, glycerol and peanut-oil droplets on the host substrates and the superamphiphobic coated substrates: (a) and (b) Al; (c) and (d): glass slide.

respectively (JCPDS Card No. 05-0667). The formation of Cu occurs through a simple redox reaction as shown in Equation (1), where the aluminium acts as a reducing agent to take Cu^{2+}. Part of the produced Cu reacted with oxygen to form Cu_2O [Equation (2)]. Fig. 2(b) shows the FTIR spectra of the superamphiphobic coatings. Bands at 1647 and 1438 cm^{-1} were respectively attributed to the asymmetrical stretching vibrations and symmetrical stretching vibrations of –COO groups of the perfluorooctanoic acid (PFOA) molecules[62]. The presence of the bands at 1138, 1208 and 1241 cm^{-1} were attributed to the –CF stretching vibrations of $–CF_2$ and $–CF_3$ groups[62,63]. The results of XRD and FTIR show that the main compositions of the superamphiphobic powder were Cu and Cu_2O cores covered with $–CF_2$ and $–CF_3$ groups which have a low surface energy and can effectively reduce the surface energy of the highly textured Cu and Cu_2O powders. The EDS spectrum shown in Fig. 2(c) also demonstrated the elements of the superamphiphobic powder with Cu and O from Cu and Cu_2O, the elements C and F were from PFOA and small amounts of Al was from the Al plate used during the aforementioned reductions [Fig. 1(a)].

$$2Al + 3Cu^{2+} \rightarrow 3Cu + 2Al^{3+} \quad (1)$$

$$4Cu + O_2 \rightarrow 2Cu_2O \quad (2)$$

The prepared superamphiphobic powder can be bonded onto hard materials via dropping the powder through a sieve on to either double sided tape or a surface pre-treated with a spray adhesive. Fig. 3 shows water, glycerol and peanut-oil droplets on the original and the bonded Al [Fig. 3(a) and (b)] and glass slide substrates [Fig. 3(c) and (d)], respectively. The superamphiphobic coatings presented here was bonded by double sided tape. The contact angles (CAs) and rolling off angles (RAs) of the samples are list in Table I. Water, glycerol and peanut-oil droplets spread onto the as-received Al and glass slide substrates, exhibiting hydrophilicity and lipophilicity. For the coated surfaces, the testing liquid droplets remained as near spheres and could easily roll off from the surfaces (see Supporting Information, Videos S1 and S2), showing excellent superhydrophobicity and superoleophobicity. The coated regions exhibited water, glycerol and peanut oil CAs of approximately 158 °, 156 ° and 153 °, respectively, irrespective of the substrate. To further test the liquid repellence of the obtained coatings, organic solvents, including diiodomethane (γ_{LV} = 50.9 mN/m[51,62]), ethylene glycol (γ_{LV} = 47.3 mN/m[51,62]) and benzyl alcohol (γ_{LV} = 38.0 mN/m[62]), were dropped on the coated glass slide surface, and the measured CAs were respectively 154.6±1.3 °, 154.0±0.8 ° and 151.2±1.6 °, and the corresponding RAs were respectively 5.8±2.1 °, 5.7±3.4 ° and 10.9±4.5 °.

Special surface micro structures (i.e. re-entrant structures) are essential for the superamphiphobicity. Here we used SEM to detect the micro structures endowed from the prepared superamphiphobic coatings. Fig. 4(a)–(d) show the top-view SEM images of the superamphiphobic coatings with different magnifications. Many irregularly shaped features with sizes ranging from several hundred nanometers to dozens of micrometers were uniformly bonded on the surface [Fig. 4(a)] and formed a rough morphology. Top-view SEM images in high magnification presented the structured morphologies with micro-nano sized features that in some locations resembled leaf shapes [Fig. 4(b)], protrusions [Fig. 4(c)] and coralline-shaped [Fig. 4(d)] structures. Fig. 4(e)–(h) show the cross-sectional-view SEM images of the superamphiphobic coatings. The coated superamphiphobic layer was about 45 µm thick, wherein some irregularly shaped micro-sized large particles were observed, as shown in Fig.4 (e). The cross-sectional-view

Table I. Contact angles (CAs) and Rolling-off angles (RAs) values of the uncoated and coated hard materials.

	Water		Glycerol		Peanut-oil	
	CA	RA	CA	RA	CA	RA
Uncoated Al	79.6±1.5°	None	71.9±1.7°	None	18.7±1.5°	None
Coated Al	158.8±1.2°	2.5±0.7°	156.5±1.1°	3.7±0.6°	152.9±1.2°	6.9±1.1°
Uncoated glass slide	32.6±0.8°	None	33.6±1.4°	None	18.7±0.3°	None
Coated glass slide	158.2±2.1°	2.1±1.3°	155.4±1.6°	4.3±1.2°	152.1±2.1°	6.8±0.8°

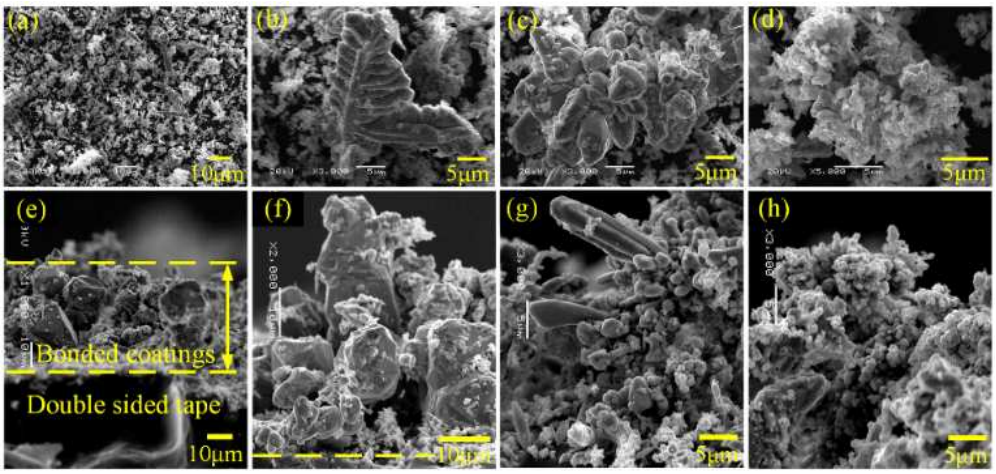

Fig. 4 (a)–(d) Top-view and (e)–(h) cross-sectional-view SEM images of the superamphiphobic coatings on glass slide.

SEM images in higher magnification in Fig. 4(f)–(h) respectively displayed three typical structures: blocky, dendritic and coralline-shaped structures. These structures are randomly agglomerated and were covered with numerous micro/nano-particles, creating micron- or submicron-sized valleys, protrusions, pits and pores. These surface textures further created re-entrant geometries at multiple scales. When exposing liquid droplets contact with the coated surfaces, the highly roughened surface structures decreased the solid-liquid interfacial interactions and the re-entrant geometries capable of trapping air at the interface construct a composite solid-liquid-air interface, a wetting behavior in the Cassie-Baxter state[64] was thereafter formed. Therefore, water, glycerol and peanut-oil droplets were supported by these surface structures as nearly spherical shapes and easily rolled off from the coated superamphiphobic surfaces. Additionally, when smooth Al plate and smooth glass slide were modified by PFOA solution, they could not behave as super-liquid repellent surfaces (see Supporting Information, Fig. S2). Thus, the presence of the powder structures is very important for the superamphiphobicity and the self-cleaning properties.

The coated surfaces maintained their superamphiphobicity after being placed in a laboratory air environment at room temperature for more than a year earlier. To further demonstrate the robustness and durability of the bonded superamphiphobic coatings, falling sand abrasion and UV irradiation tests were performed. Fig. 5(a) shows the schematic drawing of the falling sand abrasion tests. Fig. 5(b)

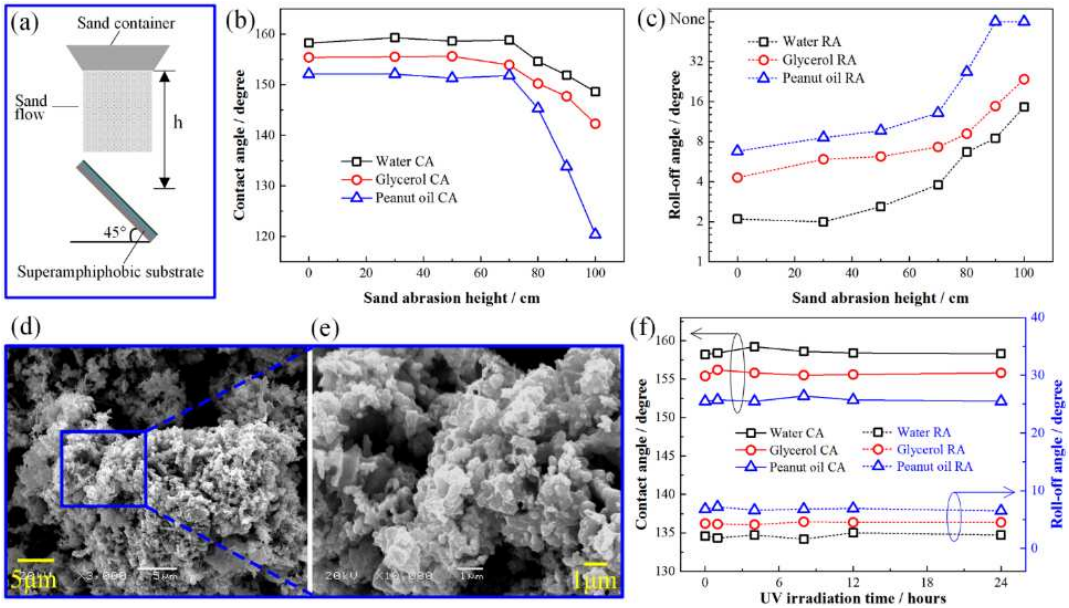

Fig. 5 Mechanical resistance and durability quantified by sand abrasion and UV irradiation. (a) Schematic drawing of a sand abrasion experiment; [(b) and (c)] Plot of water, glycerol and peanut-oil CAs and RAs after each abrasion tests for different heights of sand abrasion; [(d) and (e)] SEM images of a micro structure after sand impingement (h = 50 cm) with different magnification; (f) Water, glycerol and peanut-oil CAs and RAs of the coatings after UV irradiation (365 nm, 32 W) for different times.

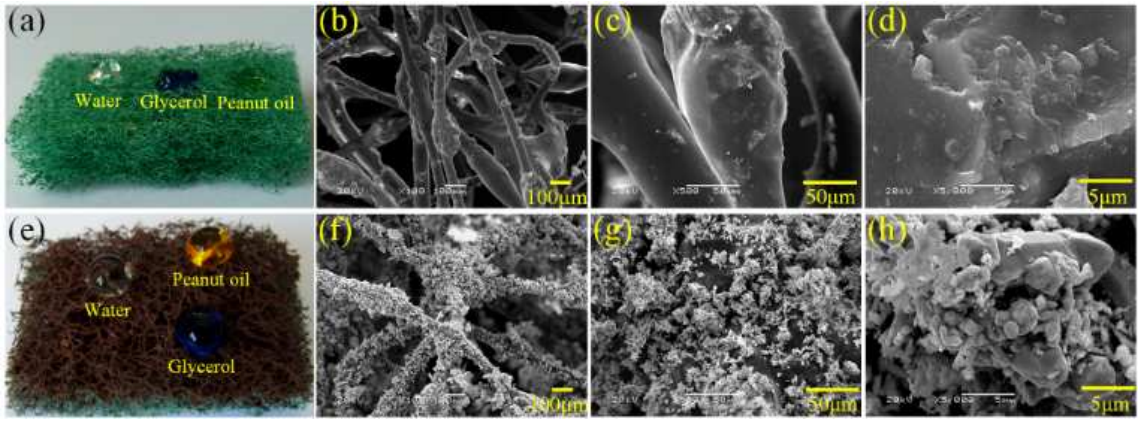

Fig. 6 Photograph of water, glycerol and peanut-oil droplets on (a) the original and (e) the coated scouring pad; SEM images of (b)–(d) the original and (f)–(h) the coated scouring pad.

and (c) respectively depict the CAs and RAs of water, glycerol and peanut-oil droplets on the coatings after sand abrasion from 0 to ~100 cm height. It clearly shows that when $h \leq$ 70 cm, though the coatings suffered from intense sand abrasion for as long as 2 min, the CAs and RAs changed little and the coatings maintained their superamphiphobicity. Video S3 shows a falling sand abrasion from a height of 50 cm (impact velocity ~3.16 m/s and impact energy ~5.65×10^{-7} to 1.07×10^{-5} J, see Supporting Information, Section S1), and Fig. 5(d) and (e) present the corresponding SEM images. The coatings were not sufficiently robust to completely resist sand impact and some micro-structures were destroyed [Fig. 5(d)]. However, zooming into the destroyed structures revealed almost unaltered coralline-shaped structures, consisting of many pits and bumps [Fig. 5(e)]. The remarkable mechanically robust performance of the superamphiphobic coatings enabled the proposed coatings to be better candidates for many applications than the majority of their counterparts previously studied in the literature, such as anti-icing[12-14,16,20]. For *h* larger than 70 cm, the impact energy was high and the microstructures of the coatings were heavily damaged (see Supporting Information, Section S1 and Fig. S3), which resulted in the CAs of the testing liquid droplets decreased rapidly and the corresponding RAs increased, indicating that the superamphiphobicity was weakened [Fig. 5(b) and (c)]. Fig. 5(f) shows the water, glycerol and peanut-oil CAs and RAs of the samples under UV exposure for different times. It clearly shows that the CAs and RAs remained similar after UV irradiation for more than 24 hours, indicating that both surface morphology and chemistry changed little after UV irradiation. The water, glycerol and peanut-oil CAs and RAs of the coatings immersed in distilled water and aqueous solution of HCl (pH=1, 0.1 mol/L), NaOH (pH=13, 0.1 mol/L) and NaCl (0.5 mol/L) for 24 h were shown in Table II. It clearly showed that the immersion in distilled water and aqueous solution of NaOH and NaCl had little influence on the wettability of the superamphiphobic coatings as the CAs and RAs almost kept unchanged. However, for the one immersed in HCl solution, it was noticed that the non-wetting property of the coatings was maintained during the first 4 h and then gradually deteriorated and after 24 h immersion the CAs for water, glycerol and peanut-oil were respectively ~143 °, 135 ° and 122 °. This may be due to the physicochemical processes during the immersion[59] which will be focused on in further studies. These results demonstrated that the obtained superamphiphobic coatings had remarkable resistances to distilled water and acidic/alkaline/saline solution invasion.

The superamphiphobic coatings were also applied to soft porous substrates by spray adhesives. Fig. 6(a) shows water, glycerol and peanut-oil droplets on the original scouring pad. For the original scouring pad, fibers with diameter of ~50 μm intersected with each other and some radial expansion (~100 μm) along the fibers were observed. Some micro-sized dome-like features were randomly distributed on the fibers

Table II. Contact angles (CAs) and Rolling-off angles (RAs) values of the coated glass slides immersed in different aqueous media for 24 h.

	Water		Glycerol		Peanut-oil	
	CA	RA	CA	RA	CA	RA
Before immersion	158.2±2.1°	2.1±1.3°	155.4±1.6°	4.3±1.2°	152.1±2.1°	6.8±0.8°
Distilled water	159.3±1.3°	2.3±0.7°	155.9±1.4°	4.8±2°	153.3±1.5°	7.8±2.1°
HCl (0.1 mol/L)	143.5±8.5°	24.5±3.7°	135.5±4.5°	None	122.8±4.8°	None
NaOH (0.1 mol/L)	157.8±1.5°	4.1±0.5°	156.0±1.5°	6.5±1.5°	153.2±2.5°	8.2±0.5°
NaCl (0.5 mol/L)	158.7±2.5°	2.0±1.5°	155.2±1.0°	5.6±1.8°	151.8±1.5°	7.1±0.5°

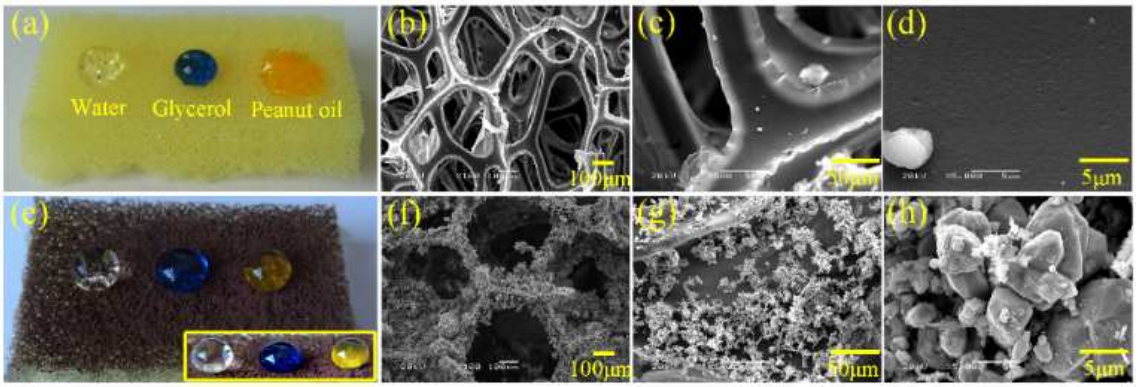

Fig. 7 Photograph of water, glycerol and peanut-oil droplets on (a) the original and (e) the coated sponge; SEM images of (b)–(d) the original and (f)–(h) the coated sponge.

[Fig. 6(b)–(d)], generating a common hydrophobic but lipophilic wettability. Water droplet stayed on the surface as a hemisphere but glycerol and peanut-oil droplets totally penetrated the untreated scouring pad. However, the coated scouring pad exhibited good liquid repellency for water, glycerol and peanut-oil by keeping the droplets near spherical shape without any penetration or adhesion (though some of the droplets were trapped in the concave structures), as shown in Fig. 6(e). The SEM images of the coated scouring pad [Fig. 6(f)–(h)] show that all the fibres were covered with superamphiphobic Cu and Cu_2O particles, preventing the testing liquids adhered to the fibres or penetrated into the substrate through the porous macrostructures.

The original sponge is hydrophilic and lipophilic, and which can be wetted by both water and oils, exhibiting poor liquid repellent properties, as shown in Fig. 7(a). After being treated with the superamphiphobic coatings, the sponge held all the liquid droplets as quasi-spheral shapes on the uppermost layer of the sponge [Fig. 7(e)] and there was no adhesion apparent as the droplets rolled off the inclined surface (see Supporting Information, Video S4). The SEM images show that the framework surfaces of the original sponge were very smooth [Fig. 7(b)–(d)]. However, after coatings, all the surfaces of the framework were highly textured and covered with superamphiphobic Cu and Cu_2O particles, as shown in Fig. 7(f)–(h).

Our coatings are also effective in converting the wetting behavior of extremely hydrophilic/oleophilic filter paper. Fig. 8(a) shows the reverse wettability between the uncoated and the coated regions of the filter paper. The uncoated region can be completely wetted by water, glycerol and peanut-oil droplets, indicating extremely hydrophilic/oleophilic properties, because of the existence of cavities [Fig. 8(b)] and abundant hydroxyl groups in filter paper structure[65]. In the magnified SEM images of uncoated filter paper [Fig. 8(c) and (d)], numerous longitudinal corrugations along the paper fiber with diameters of ~25 μm and a few micro-scale particles were observed. However, after coating, the paper fibers were almost all covered with superamphiphobic Cu and Cu_2O particles [Fig. 8(e)–(g)]. The filter paper covered with the superamphiphobic coatings cannot be wetted by water or oils [Fig. 8(a)] and presented outstanding superamphiphobicity. The CAs of water, glycerol and peanut-oil were respectively 159.3±3.4 °, 156.9±3.6 ° and 154.2±2.5 °, and the droplets could also roll off from the coated surfaces easily (see Supporting Information, Video S5).

Creating oil repellent surfaces on stretchy substrates that work under liquid environments is an important and

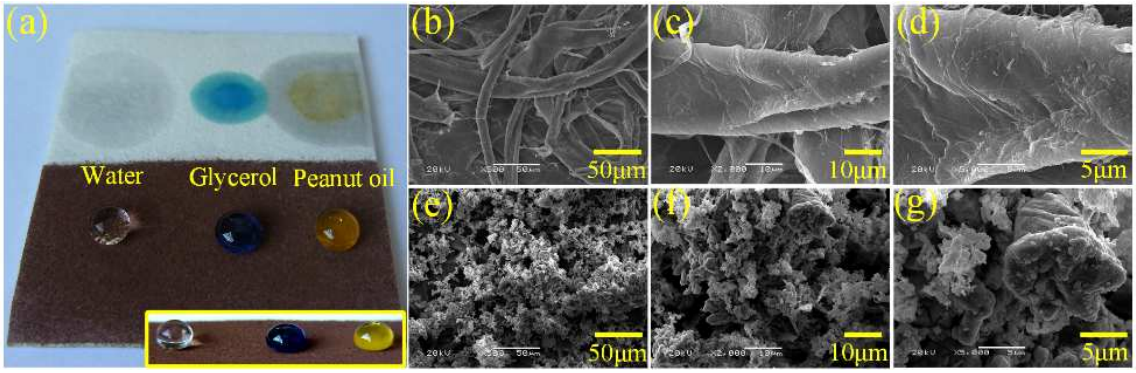

Fig. 8 Photograph of water, glycerol and peanut-oil droplets on (a) the original and (e) the coated filter paper; SEM images of (b)–(d) the original and (f)–(h) the coated filter paper.

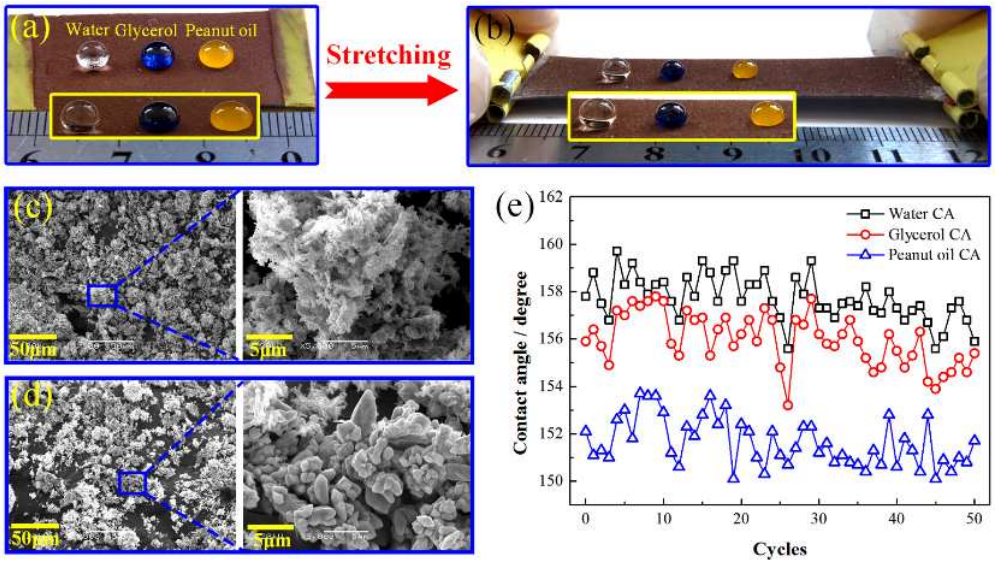

Fig. 9 Photograph of water, glycerol and peanut-oil droplets on coated rubber (a) before and (b) after stretching; SEM images of the coated rubber (c) before and (d) after stretching; (e) Plot of water, glycerol and peanut-oil contact angles after each stretch and release cycle.

challenging work since the deformation of the stretchy substrates would "dilute" and even damage the surface structures. In order to show our superamphiphobic coatings are suitable to stretchy substrates, we used a piece of rubber (3.0 cm in length) as the substrate and superamphiphobic coatings were bonded by sprayed adhesive. Fig. 9(a) and (c) show the photos of water, glycerol and peanut-oil droplets on the coated rubber before and after stretching, respectively. It clearly shows that the three liquid droplets on the surface were close to spherical and easily rolled off even after being stretched to double the original length of rubber (see Supporting Information, Video S6). Fig. 9(b) and (d) respectively shows the SEM images of the superamphiphobic coatings before and after stretching. Compared with Fig. 4, although the microstructures were distributed sparsely after being stretched by mechanical stress, the surface micro-morphologies did not change much, which enabled the coated surfaces to retain their superamphiphobicity. The water, glycerol and peanut-oil CAs during 50 cycles of stretching and releasing test remained above 150 °, as shown in Fig. 9(e). Thus it was demonstrated that the superamphiphobicity was maintained even after stretching and releasing for more than 50 cycles (see Supporting Information, Video S6), which demonstrated the possibility to build robust superamphiphobic surfaces on stretchy substrates.

4. Conclusions

In summary, we reported a facile method to fabricate superamphiphobic coatings with CAs for different liquids (water, glycerol, peanut-oil and some organic solvents) all in excess of 150 ° and RAs lower than 10 °. The superamphiphobic coatings were obtained by chemical deposition and subsequent surface coating with fluorination and could be easily coated on both hard (metal and glass) and soft materials (scouring pad, sponge, filter paper and rubber) via adhesives. The superamphiphobic coatings possessed excellent mechanical robustness and durability, such as remarkable resistances to falling sand abrasion, UV irradiation, distilled water and acidic/alkaline/saline solution invasion. A multi-cycle stretch-release method was developed to test the robustness of self-cleaning soft flexible materials. The treated rubber surprisingly remained superamphiphobicity even after 50 cycles of stretch-release tests. These results demonstrate that the new coatings can be readily applied to a wide range of materials to produce extremely durable superamphiphobic coatings that maintain both oil and water repulsion even after intense UV-exposure, multiple stress-strain cycles, sand abrasion and strong solution invasion.

Acknowledgements

This work was financially supported by National Natural Science Foundation of China (NSFC, Grant No. 90923022), the Fundamental Research Funds for the Central Universities (DUT15RC(3)066) and an Innovation and Creativity Fund for Doctoral Students Granted by Science & Technology Review (Grant No. KJDB2012010).

References

1 W. Dong, W. Jian-Nan, W. Si-Zhu, C. Qi-Dai, Z. Shuai, Z. Hao, S. Hong-Bo, and J. Lei, *Adv. Funct. Mater.*, 2011, **21**, 2927.
2 S. G. Lee, H. S. Lim, D. Y. Lee, D. Kwak, and K. Cho, *Adv. Funct. Mater.*, 2013, **23**, 547.
3 W. Barthlott and C. Neinhuis, *Planta*, 1997, **202**, 1.

4 L. Zhai, M. C. Berg, F. C. Cebeci, Y. Kim, J. M. Milwid, M. F. Rubner, and R. E. Cohen, *Nano Lett.*, 2006, **6**, 1213.
5 X. Gao and L. Jiang, *Nature*, 2004, **432**, 36.
6 F. Xia and L. Jiang, *Adv. Mater.*, 2008, **20**, 2842.
7 K. Liu and L. Jiang, *Nano Today*, 2011, **6**, 155.
8 K. Liu and L. Jiang, *ACS Nano*, 2011, **5**, 6786.
9 J. Chapman and F. Regan, *Adv. Eng. Mater.,* 2012, **14**, B175.
10 H. Zhang, R. Lamb and J. Lewis, *Sci. Technol. Adv. Mater.*, 2005, **6**, 236.
11 X. Zhang, F. Shi, J. Niu, Y. Jiang and Z. Wang, *J. Mater. Chem.*, 2008, **18**, 621.
12 S. A. Kulinich and M. Farzaneh, *Langmuir*, 2009, **25**, 8854.
13 S. A. Kulinich, S. Farhadi, K. Nose and X. W. Du, *Langmuir,* 2011, **27**, 25.
14 S. Farhadi, M. Farzaneh and S. A. Kulinich, *Appl. Surf. Sci*., 2011, **257**, 6264.
15 S. A. Kulinich and M. Farzaneh, *Appl. Surf. Sci.,* 2009, **255**, 8153.
16 A. Lazauskas, A. Guobienė, I. Prosyčevas, V. Baltrušaitis, V. Grigaliūnas, P. Narmontas and J. Baltrusaitis, *Mater. Charact.,* 2013, **82**, 9.
17 K. K. Varanasi, T. Deng, J. D. Smith, M. Hsu, and N. Bhate, *Appl. Phys. Lett.*, 2010, **97**, 234102.
18 X. Yao, Y. Song and L. Jiang, *Adv. Mater.*, 2011, **23**, 719.
19 P. Guo, Y. Zheng, M. Wen, C. Song, Y. Lin, and L. Jiang, *Adv. Mater.*, 2012, **24**, 2642.
20 L. B. Boinovich, A. M. Emelyanenko, V. K. Ivanov, and A. S. Pashinin, *ACS Appl. Mater. Interfaces*, 2013, **5**, 2549.
21 Y. Chen, Y. Zhang, L. Shi, J. Li, Y. Xin, T. Yang, and Z. Guo, *Appl. Phys. Lett.*, 2012, **101**, 33701.
22 X. Zhang, Z. Li, K. Liu, and L. Jiang, *Adv. Funct. Mater.*, 2013, **23**, 2881.
23 Y. Lu, S. Sathasivam, J. Song, C. R. Crick, C. J. Carmalt, and I. P. Parkin, *Science*, 2015, **347**, 1132.
24 J. Song, S. Huang, Y. Lu, X. Bu, J. E. Mates, A. Ghosh, R. Ganguly, C. J. Carmalt, I. P. Parkin, W. Xu, and C. M. Megaridis, *ACS Appl. Mater. Interfaces*, 2014, **6**, 19858.
25 Y. Lu, S. Sathasivam, J. Song, F. Chen, W. Xu, C. J. Carmalt, and I. P. Parkin, *J. Mater. Chem. A*, 2014, **2**, 11628.
26 C. Duan, T. Zhu, J. Guo, Z. Wang, X. Liu, H. Wang, X. Xu, Y. Jin, N. Zhao, and J. Xu, *ACS Appl. Mater. Interfaces*, 2015, **7**, 10475.
27 W. Xu, J. Song, J. Sun, Y. Lu, and Z. Yu, *ACS Appl. Mater. Interfaces*, 2011, **3**, 4404.
28 Z. Wang, Q. Li, Z. She, F. Chen, and L. Li, *J. Mater. Chem.*, 2012, **22**, 4097.
29 K. C. Chang, H. I. Lu, C. W. Peng, M. C. Lai, S. C. Hsu, M. H. Hsu, Y. K. Tsai, C. H. Chang, W. I. Hung, Y. Wei, and J. M. Yeh, *ACS Appl. Mater. Interfaces*, 2013, **5**, 1460.
30 P. Auad, E. Ueda and P. A. Levkin, *ACS Appl. Mater. Interfaces*, 2013, **5**, 8053.
31 M. Toma, G. Loget and R. M. Corn, *ACS Appl. Mater. Interfaces*, 2014, **6**, 11110.
32 F. Chen, W. Xu, Y. Lu, J. Song, S. Huang, L. Wang, I. P. Parkin, and X. Liu, *Micro Nano Lett.*, 2015, **10**, 105.
33 M. Elsharkawy, T. M. Schutzius and C. M. Megaridis, *Lab Chip*, 2014, **14**, 1168.
34 A. Ghosh, R. Ganguly, T. M. Schutzius, and C. M. Megaridis, *Lab Chip*, 2014, **14**, 1538.
35 F. Lapierre, M. Harnois, Y. Coffinier, R. Boukherroub, and V. Thomy, *Lab Chip*, 2014, **14**, 3589.
36 H. Butt, C. Semprebon, P. Papadopoulos, D. Vollmer, M. Brinkmann, and M. Ciccotti, *Soft Matter*, 2012, **9**, 418.
37 Y. Lu, J. Song, X. Liu, W. Xu, Y. Xing, and Z. Wei, *ACS Sustainable Chem. Eng.*, 2013, **1**, 102.
38 A. Tuteja, W. Choi, M. Ma, J. M. Mabry, S. A. Mazzella, G. C. Rutledge, G. H. McKinley, and R. E. Cohen, *Science*, 2007, **318**, 1618.
39 A. Tuteja, W. Choi, G. H. McKinley, R. E. Cohen, and M. F. Rubner, *MRS Bull.*, 2008, **33**, 752.
40 W. Choi, A. Tuteja, S. Chhatre, J. M. Mabry, R. E. Cohen, and G. H. McKinley, *Adv. Mater.*, 2009, **21**, 2190.
41 Y. Liu, Y. Xiu, D. W. Hess, and C. P. Wong, *Langmuir*, 2010, **26**, 8908.
42 J. Song, S. Huang, K. Hu, Y. Lu, X. Liu, and W. Xu, *J. Mater. Chem. A*, 2013, **1**, 14783.
43 V. A. Ganesh, S. S. Dinachali, A. S. Nair, and S. Ramakrishna, *ACS Appl. Mater. Interfaces*, 2013, **5**, 1527.
44 Z. Geng, J. He, L. Xu, and L. Yao, *J. Mater. Chem. A*, 2013, **1**, 8721.
45 H. Bellanger, T. Darmanin, E. T. de Givenchy, and F. Guittard, *Chem. Rev.*, 2014, **114**, 2694.
46 H. Zhao and K. Law, *ACS Appl. Mater. Interfaces*, 2012, **4**, 4288.
47 T. L. Liu and C. J. Kim, *Science*, 2014, **346**, 1096.
48 J. Xi, L. Feng and L. Jiang, *Appl. Phys. Lett*., 2008, **92**, 53102.
49 H. Zhou, H. Wang, H. Niu, A. Gestos, and T. Lin, *Adv. Funct. Mater.*, 2013, **23**, 1664.
50 L. Xiong, L. L. Kendrick, H. Heusser, J. C. Webb, B. J. Sparks, J. T. Goetz, W. Guo, C. M. Stafford, M. D. Blanton, S. Nazarenko, and D. L. Patton, *ACS Appl. Mater. Interfaces*, 2014, **6**, 10763.
51 X. Deng, L. Mammen, H. J. Butt, and D. Vollmer, *Science*, 2012, **335**, 67.
52 X. Deng, L. Mammen, Y. Zhao, P. Lellig, K. Müllen, C. Li, H. Butt, and D. Vollmer, *Adv. Mater.*, 2011, **23**, 2962.
53 T. M. Schutzius, I. S. Bayer, J. Qin, D. Waldroup, and C. M. Megaridis, *ACS Appl. Mater. Interfaces*, 2013, **5**, 13419.
54 Z. Xu, Y. Zhao, H. Wang, X. Wang, and T. Lin, *Angew. Chem. Int. Ed.*, 2015, **54**, 4527.
55 S. G. Lee, D. S. Ham, D. Y. Lee, H. Bong, and K. Che, *Langmuir*, 2013, **29**, 15051.
56 R. G. Karunakaran, C. Lu, Z. Zhang, and S. Yang, *Langmuir*, 2011, **27**, 4594.
57 T. Verho, C. Bower, P. Andrew, S. Franssila, O. Ikkala, and R. H. A. Ras, *Adv. Mater.*, 2011, **23**, 673.
58 S. A. Kulinich, M. Honda, A. L. Zhu, A. G. Rozhin and X. W. Du, *Soft Matter,* 2015, **11**, 856.

59 L. Boinovich and A. Emelyanenko, *Adv. Colloid Interface Sci.*, 2012, **179**, 133.
60 J. Zhang, B. Li, L. Wu, and A. Wang, *Chem. Commun. (Camb)*, 2013, **49**, 11509.
61 F. Xue, D. Jia, Y. Li and X. Jing, *J. Mater. Chem. A*, 2015, **3**, 13856.
62 X. Zhu, Z. Zhang, X. Xu, X. Men, J. Yang, X. Zhou and Q. Xue, *J. Colloid Interface Sci.*, 2013, **5**, 13419.
63 X. Xu, Z. Zhang and W. Liu, *Colloids Surfaces A: Physicochem. Eng. Aspects*, 2009, **341**, 21.
64 X. Li, P. Zhang, L. Jin, T. Shao, Z. Li, and J. Cao, *Environ. Sci. Technol.*, 2012, **46**, 5528.
65 A. B. D. Cassie and S. Baxter, *T. Faraday Soc.*, 1944, **40**, 546.
66 X. Huang, X. Wen, J. Cheng, and Z. Yang, *Appl. Surf. Sci.*, 2012, **258**, 8739.

Graphical Abstract